GEOPHYSICAL RESEARCH LETTERS, VOL. 37, L24806, doi:10.1029/2010GL045902, 2010

Infrared sounding of the trade-wind boundary layer: AIRS and the RICO experiment

João P. A. Martins,[1] João Teixeira,[2] Pedro M. M. Soares,[1] Pedro M. A. Miranda,[1] Brian H. Kahn,[2] Van T. Dang,[2] Frederick W. Irion,[2] Eric J. Fetzer,[2] and Evan Fishbein[2]

Received 22 October 2010; accepted 3 November 2010; published 22 December 2010.

[1] The new generation of remote sensors on board NASA's A-Train constellation offers the possibility of observing the atmospheric boundary layer in different regimes, with or without clouds. In this study we use data from the Atmospheric InfraRed Sounder (AIRS) and of the Rain In Cumulus over the Ocean (RICO) campaign, to verify the accuracy and precision of the AIRS Version 5 Level 2 support product. This AIRS product has an improved vertical sampling that is necessary for the estimation of boundary layer properties. Good agreement is found between AIRS and RICO data, in a regime of oceanic shallow cumulus that is known to be difficult to analyze with other remote sensing data, and also shows a low sensitivity to cloud or land fraction. This suggests that AIRS data may be used for global boundary layer studies to support parameterization development in regions of difficult in-situ observation. **Citation:** Martins, J. P. A., J. Teixeira, P. M. M. Soares, P. M. A. Miranda, B. H. Kahn, V. T. Dang, F. W. Irion, E. J. Fetzer, and E. Fishbein (2010), Infrared sounding of the trade-wind boundary layer: AIRS and the RICO experiment, *Geophys. Res. Lett.*, *37*, L24806, doi:10.1029/2010GL045902.

1. Introduction

[2] The planetary boundary layer (PBL) plays a key role in climate by mediating the interactions between the free troposphere and the land-ocean-ice surface. In spite of its importance, parameterizations of PBL physics in climate and weather prediction models are still not realistic enough for accurate predictions of these interactions [e.g., *Teixeira et al.*, 2008]. Shallow convective boundary layers are the most common type of PBL over the subtropical oceans, and their role is essential to understand the tropical general circulation [e.g., *Riehl et al.*, 1951; *Stevens*, 2005]. Trade wind boundary layer clouds are also believed to play an essential role in climate change, as several studies suggest that differences in model climate sensitivities can largely be explained by the models' differences in representation of PBL clouds [*Bony and Dufresne*, 2005; *Wyant et al.*, 2006].

[3] The height of the boundary layer, typically marked by sharp temperature and humidity vertical gradients, is an important integrated measure of the PBL properties and is often a key parameter in turbulence parameterizations. Given its characteristics, the cloudy PBL is remarkably difficult to observe with space-borne instruments. Only a few studies have examined the ability of remote sensing instruments to measure PBL properties, largely because of poor vertical resolution and cloud opacity in the infrared [e.g., *von Engeln et al.*, 2005]. Techniques that rely on cloud opacity to the infrared have been used to estimate cloud top heights, and they provide a good indirect estimate for PBL height in regions dominated by low clouds [e.g., *Wood and Bretherton*, 2004; *Zuidema et al.*, 2009]. While these estimates assume a simple mean thermodynamical profile that can account for a mean decoupling between cloudy and dry layers, variability in the coupling is not accounted for. Perhaps more importantly, the retrievals are restricted to completely overcast, opaque footprints. In contrast, techniques relying on the full knowledge of the cloud-cleared thermodynamical profiles allow direct estimations of PBL height, since it maybe defined as the level where their gradients are largest [e.g., *Fetzer et al.*, 2004]. Recent studies show that even in the presence of significant cloudiness, biases in temperature and water vapor are not significantly increased [*Wu*, 2009; *Susskind et al.*, 2010], despite the reduced sampling frequency [*Fetzer et al.*, 2006].

[4] In this work, lower tropospheric profiles from a less often used Atmospheric InfraRed Sounder (AIRS) dataset [*Aumann et al.*, 2003], referred to as the Level 2 (L2) Support product, is compared to observations from the Rain in Cumulus over the Ocean (RICO) campaign [*Rauber et al.*, 2007]. The former consists of 100-levels atmospheric retrievals with a nominal grid spacing of about 25 hPa in the PBL, whereas the more commonly used 28 level standard product has only 4 levels below 700 hPa [*Susskind et al.*, 2006]; neither product has been extensively validated over the global oceans. The main goal of this study is to quantify the ability of AIRS to reproduce the main thermodynamic properties of the PBL in trade wind regions. This is the type of low cloud fraction regime where the AIRS observations and retrieval algorithm are designed to have optimal sampling frequency and low retrieval biases, since it relies on cloud free pixels [*Fetzer et al.*, 2004]. Also, the presence of temperature gradients increases the reliability of the measurements [*Maddy and Barnet*, 2008; *Liang et al.*, 2010], so that the information content derived from the radiances should be larger near the PBL top. There is evidence that the averaging kernels from the Version 5 (V5) AIRS retrievals may be too broad for T and q (temperature and water vapor mixing ratio, respectively) [*Pougatchev*, 2008; N. Pougatchev, personal communication, 2010]. In fact, AIRS may resolve

[1]CGUL, IDL, University of Lisbon, Lisbon, Portugal.
[2]Jet Propulsion Laboratory, California Institute of Technology, Pasadena, California, USA.

0094-8276/10/2010GL045902

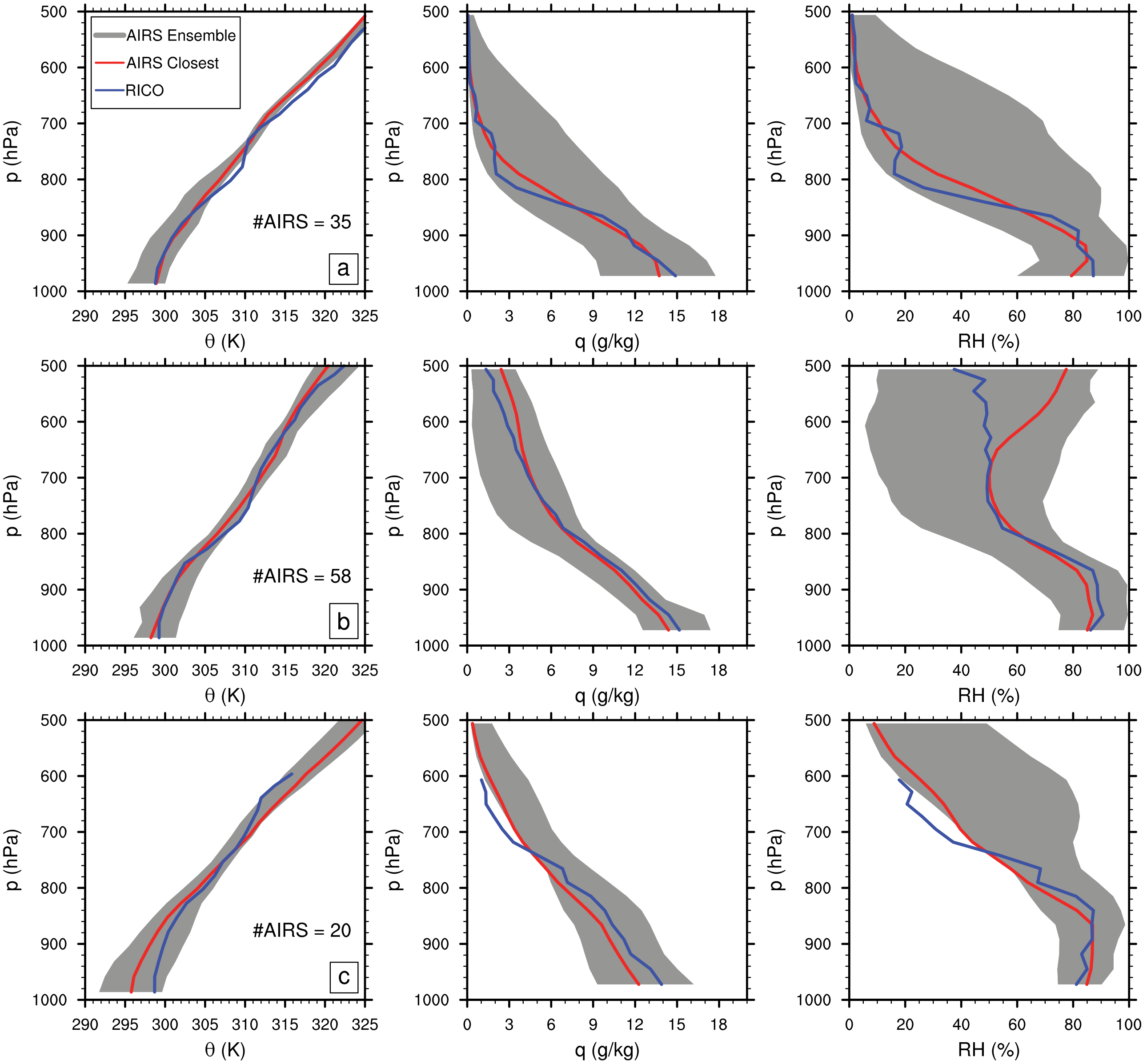

Figure 1. Three examples of realistic AIRS retrievals: (a) Seward Johnson Research Vessel rawinsonde, launched 23 January 2005 16UTC NNE off Barbuda, (b) Spanish Point (Barbuda) rawinsonde, launched 6 January 2005 17 UTC, and (c) C130 dropsonde released 16 January 2005 16 UTC ENE off Barbuda. In blue, the rawinsonde; in red the AIRS sounding geographically closest to the sonde and in shade the ensemble of AIRS soundings that match the rawinsonde. The number of AIRS soundings using in each case is also shown. By coincidence, the number is the same for temperature and moisture in these cases.

more finely vertical variations within the PBL than currently reported [*Maddy and Barnet*, 2008], which further motivates comparisons to correlative in situ observations such as those from RICO.

2. Data and Methods

[5] The RICO campaign took place near the Caribbean Islands of Antigua and Barbuda, within the western Atlantic trade wind region, between 24 November 2004 and 25 January 2005. The main goal of the campaign was to assess the importance of precipitation on the genesis of trade wind clouds and its role on the global circulation of the atmosphere [*Nuijens et al.*, 2009; *Snodgrass et al.*, 2009]. This study uses data from the rawinsondes launched from Spanish Point (Barbuda) and from the Research Vessel Seward Johnson, and dropsondes from the National Science Foundation (NSF) – National Center for Atmospheric Research (NCAR) C130 aircraft, as they provide a high resolution sample of lower tropospheric profiles of temperature and moisture.

[6] The RICO data was interpolated to the AIRS L2 Support pressure levels using a moving average filter with a length corresponding to the 25 hPa grid spacing, and all

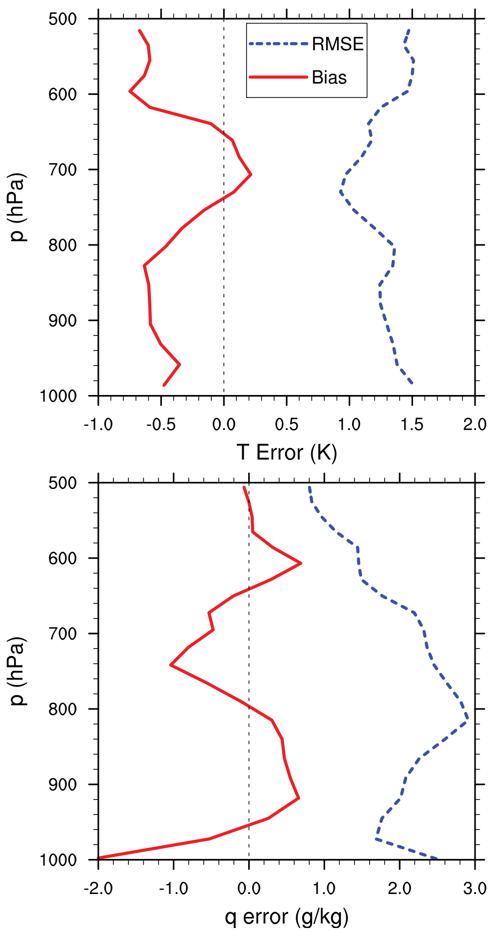

Figure 2. In red, the bias (AIRS-RICO) and in blue, the root mean square error (RMSE) profiles for temperature, on the top (in K) and water vapor mixing ratio at the bottom (in g/kg).

AIRS soundings closer than 3° to Spanish Point were retrieved. From this set, only those between ±3 hours before and after each RICO sonde launch were considered. Applying these criteria, each RICO sonde has an ensemble of between 4 and 143 matching AIRS soundings. AIRS quality flags were applied to all matched comparisons. Humidity profiles flagged with Qual_H2O = 2 ("Do not use") were excluded, as well as profiles that contain values of *RH* > 100%, *RH* being the relative humidity, due to retrieval noise either in temperature and/or specific humidity. For both profiles (humidity and temperature) only the pressure levels less than or equal to the quality control parameter "PGood" were used (pressure levels higher than this value are considered of "poor" quality). Also, RICO sondes with at least one *RH* value above 95% are excluded since it is considered that they were in the vicinity of clouds. From a total of 138 RICO sondes, 26 were disregarded due to these criteria. AIRS and RICO have significantly different sampling properties. An AIRS sounding represents the mean cloud-cleared state of an area ~45 km wide, and has coarser vertical resolution than the ~10 m typical of rawinsondes/dropsondes. A sonde may sample horizontal distances of comparable size to AIRS due to wind drift, and in fact may drift among multiple AIRS pixels, but it resolves local features such as individual trade cumulus clouds. As a consequence, we expect smoother profiles from AIRS. The availability of an ensemble of AIRS profiles for each RICO sonde is useful to quantify the horizontal structure of the PBL as a possible source for the mismatch between the two datasets.

3. Results

3.1. Thermodynamic Profiles and Error Statistics

[7] Figure 1 shows three examples of AIRS retrievals of lower-tropospheric profiles of potential temperature θ, q, and *RH* together with its corresponding RICO sonde profiles, along with the AIRS matchup (ensemble). The AIRS profiles are generally smoother than those from the sondes, as expected. However, despite some localized features, the sonde measurements are well reproduced by the AIRS ensemble (the individual RICO profile is mostly contained within the envelope of the AIRS ensemble data), and in particular, by the geographically closest AIRS retrieval. Most importantly, and most strikingly in the *RH* plots, AIRS is capable of reproducing the key features of the cloudy PBL, namely the correct height of the PBL inversion separating the two distinct layers of the troposphere, and the moist nature of the cloudy PBL. Note that the trade wind inversion is not as pronounced in RICO as it appeared in previous campaigns like BOMEX [*Siebesma et al.*, 2003]. The spread of the AIRS retrievals, represented by the shaded areas in Figure 1, also indicates that the AIRS system is capable of observing significant spatial variability within the selected area, indicating that the profiles are not just a by-product of a first guess taken from a monthly mean climatology. Details of the AIRS algorithms are described by *Susskind et al.* [2010].

[8] The overall agreement between AIRS and RICO sondes may be characterized by its coefficients of determination (defined as $R^2 = b^2 \sum\left(RICO_k - \overline{RICO}\right)^2 / \sum\left(AIRS_k - \overline{AIRS}\right)^2$, where b is the slope of the linear regression between AIRS and RICO [*Wilks*, 1995]), with computed values of 0.973 in the case of T, 0.823 for q, and 0.599 for *RH*. To characterize the height-dependence of the errors of the AIRS retrievals for all matched AIRS-RICO comparisons, two error estimates are shown in Figure 2: bias (AIRS − RICO) and root mean square error (RMSE). In the case of T, a negative AIRS bias of around −0.5 K is observed throughout the column except just above the PBL top around 700 hPa. It is reassuring that the PBL T bias is similar to the bias in the sub-tropical free troposphere where AIRS is expected to be particularly reliable [e.g., *Susskind et al.*, 2010]. The AIRS T RMSE is between 1.0–1.5 K with a minimum near 700 hPa that coincides with a minimum in the AIRS bias just above the shallow cumulus cloud tops.

[9] In the case of q profiles, absolute errors are larger at lower levels. The bias oscillates between roughly −2 and 1 g kg^{-1} from the surface to around 600 hPa, with a consistent pattern of AIRS overestimation within the PBL (from 950–800 hPa) and underestimation just above the PBL top. The q RMSE is around 2 g kg^{-1} within the PBL - between around 1.5 g kg^{-1} close to the surface and a peak of almost 3 g kg^{-1}at the mean PBL inversion height, around 800 hPa. Close to the PBL inversion, large gradients of q cause the perceived large variability in RMSE. Note that

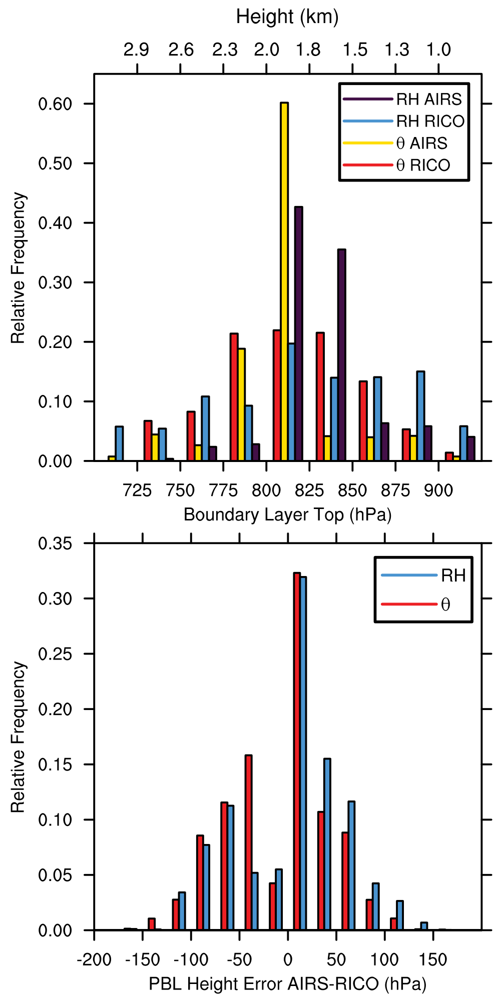

Figure 3. (top) Histograms of the PBL height using all the available AIRS and RICO sondes, for *RH* and θ. In the top axis, an estimate of the corresponding height is given. (bottom) Error histograms for *RH* and θ, obtained by calculating the differences between the PBL height given by AIRS minus its RICO corresponding value.

both the q bias and RMSE are not significantly larger in the PBL than in the free troposphere around 700 hPa, showing that the relative biases are much smaller in the moist PBL compared to the drier free troposphere. The biases and RMSE values are consistent with prelaunch requirements of the AIRS retrieval algorithm [e.g., *Goldberg et al.*, 2003; *Divakarla et al.*, 2006; *Susskind et al.*, 2010].

3.2. Possible Error Sources

[10] To better understand a few potential error sources, a vertically integrated bias (AIRS − RICO) was computed for each T and q profile from the surface up to 500 hPa. This measure was compared to AIRS retrievals of low cloud fraction (CF) and outgoing longwave radiation (OLR) to investigate possible cloud contamination problems, land fraction (LF) to quantify surface impacts on the retrievals and also the horizontal distance between the RICO sonde and the corresponding AIRS profile to quantify the T and q heterogeneity in the study area. All these factors are known to increase the apparent error of the AIRS data [e.g., *Divakarla et al.*, 2006; *Susskind et al.*, 2010] and CF, LF and OLR are part of the AIRS L2 Support dataset (results were not included here for the sake of brevity). In summary, no significant correlations were found between any of these variables and the errors (bias and RMSE), although a few of the largest errors are associated with the largest distances and smaller OLR (increase in clouds). However, these conclusions are limited by the dynamic range of the controlling parameters in the set: LF only varies between 0–0.40, CF varies between 0–0.9, and OLR is mostly in a range 200–320 Wm^{-2}. The distance between the profiles has essentially no effect. This is likely a consequence of the horizontal homogeneity of the shallow convection regime, and confirms that that the co-location procedure was robust for this comparison.

3.3. Boundary Layer Height

[11] The main advantage of using the AIRS L2 Support product is the increase in detail in the representation of the vertical structure of the atmosphere. For typical convective boundary layers over the ocean, the PBL height can be defined as the height of strong gradients in both θ and *RH*. The algorithm developed here locates the first occurrence of a gradient, ascending from the surface, that exceeds a given threshold (−0.06 K hPa^{-1} for θ and 0.4% hPa^{-1} for *RH*). Sometimes such a gradient does not exist; in which case the largest gradient is assumed to coincide with the PBL height. Only levels between 925 and 700 hPa are considered. Histograms for the PBL depth as determined by all the available AIRS and RICO sondes are presented in Figure 3. The histograms for AIRS PBL height using both θ and *RH* in Figure 3 are qualitatively similar to each other. Also, the mean value of PBL height from the AIRS retrievals (around 800 hPa) is close to the climatological value of PBL height in the trade-wind regions of *Rauber et al.* [2007]. The standard deviation of the PBL height as determined by the AIRS soundings is about 33 hPa, which is similar to the vertical gridding of the L2 Support product. The distributions of the AIRS estimates of PBL height show a mean bias of around −6 hPa and an RMSE of around 53 hPa using θ profiles, and a bias of 8 hPa and an RMSE of 56 hPa using *RH* profiles. Furthermore, the PBL gradients as given by the filtered RICO sondes are also reasonably well reproduced by AIRS, and have typical mean values close to the thresholds used in the PBL determination algorithm (not shown). The skewness of the distributions is however much different in the two datasets, and it reveals that AIRS is not able to reproduce the largest gradients revealed by RICO, which may explain the broadness of the AIRS PBL height histograms. Still, given the capabilities of the AIRS suite, these results are promising and this analysis should be extended to future in situ field campaigns to characterize both similar and dissimilar cloud regimes.

4. Conclusions

[12] This work characterizes the vertical thermodynamic structure of trade wind boundary layers using retrievals from the Atmospheric Infrared Sounder (AIRS). The fine vertical gridding (~25 hPa) of the AIRS L2 Support product is evaluated against in-situ observations from the Rain in

Cumulus over the Ocean (RICO) experiment. Essential features of the thermodynamic structure in the RICO sondes are well reproduced by the AIRS retrievals. The temperature (*T*) and specific humidity (*q*), and relative humidity (*RH*) error structures (bias and RMSE) are comparable within the PBL and the free troposphere above the PBL, where AIRS is believed to be most reliable. The reduced biases near the PBL cloud top indicate a possible relationship between bias and the vertical gradient of *T* and *q*. Generally, the error estimates for the trade wind PBL meet or exceed the pre-launch requirements of the AIRS suite, and are consistent with previous studies. Furthermore, these estimates are not particularly sensitive to cloud fraction, land fraction, outgoing longwave radiation and distance between the AIRS profile and the RICO sonde. Thus, the vertical profiles of *T* and *q*, within trade cumulus regimes similar to RICO, can be reliably used to quantify the vertical thermodynamic structure of the lower troposphere, and in particular the PBL height.

[13] A recent study by *Karlsson et al.* [2010] compared results from Multiangle Imaging Spectroradiometer (MISR), the AIRS standard product against model and reanalysis results in a transect across the Eastern Pacific. Good agreement between all the estimates was found in regions dominated by stratiform low clouds, whereas in the trade region the variability of cloud top heights increases the uncertainty of MISR estimations. AIRS should be able to produce reliable profiles in regions with little cloud cover such as the trades. AIRS also has the advantage of relatively good balance between temporal and spatial coverage and spatial resolution, in contrast to the high vertical resolution but poor horizontal resolution of the Global Positioning System Radio Occultation (GPS RO) [*von Engeln et al.*, 2005] or overall coverage of spaceborne LIDAR or MISR.

[14] However, a shortcoming of the AIRS vertical resolution is related to the ability of detecting the local variability of PBL height, since its value is close to the vertical resolution of the instrument. For this purpose, a dataset with higher resolution, especially within the PBL, would be desirable. Nevertheless, this study still suggests that this AIRS dataset has the potential to provide reliable PBL height information also beyond the trade-wind regions, as it contains global observations of the PBL structure that are useful for both spatial and seasonal variability studies, and for climate and numerical weather prediction model evaluations.

[15] **Acknowledgments.** JM is thankful to L. Nuijens, I. Trigo and C. Liang for discussions and comments on earlier versions of this paper. We would also like to thank P. Zuidema and an anonymous reviewer for their comments that greatly improved this manuscript. This work was partially funded by the Portuguese Science Foundation (FCT) under the grant SFRH/BD/37800/2007 and under Project REWRITE - PTDC/CLI/73814/2006, co-financed by the European Union under Program FEDER. JT acknowledges the support of the NASA MAP program and the Office of Naval Research. Part of the research described in this publication was carried out at the Jet Propulsion Laboratory, California Institute of Technology, under a contract with the National Aeronautics and Space Administration.

References

Aumann, H. H., et al. (2003), AIRS/AMSU/HSB on the aqua mission: Design, science objectives, data products, and processing systems, *IEEE Trans. Geosci. Remote Sens.*, *41*(2), 253–264, doi:10.1109/TGRS.2002.808356.

Bony, S., and J.-L. Dufresne (2005), Marine boundary layer clouds at the heart of tropical cloud feedback uncertainties in climate models, *Geophys. Res. Lett.*, *32*, L20806, doi:10.1029/2005GL023851.

Divakarla, M. G., C. D. Barnet, M. D. Goldberg, L. M. McMillin, E. Maddy, W. Wolf, L. Zhou, and X. Liu (2006), Validation of Atmospheric Infrared Sounder temperature and water vapor retrievals with matched radiosonde measurements and forecasts, *J. Geophys. Res.*, *111*, D09S15, doi:10.1029/2005JD006116.

Fetzer, E. J., J. Teixeira, E. T. Olsen, and E. F. Fishbein (2004), Satellite remote sounding of atmospheric boundary layer temperature inversions over the subtropical eastern Pacific, *Geophys. Res. Lett.*, *31*, L17102, doi:10.1029/2004GL020174.

Fetzer, E. J., B. H. Lambrigtsen, A. Eldering, H. H. Aumann, and M. T. Chahine (2006), Biases in total precipitable water vapor climatologies from Atmospheric Infrared Sounder and Advanced Microwave Scanning Radiometer, *J. Geophys. Res.*, *111*, D09S16, doi:10.1029/2005JD006598.

Goldberg, M. D., Y. N. Qu, L. M. McMillin, W. Wolf, L. H. Zhou, and M. Divakarla (2003), AIRS near-real-time products and algorithms in support of operational numerical weather prediction, *IEEE Trans. Geosci. Remote Sens.*, *41*(2), 379–389, doi:10.1109/TGRS.2002.808307.

Karlsson, J., G. Svensson, S. Cardoso, J. Teixeira, and S. Paradise (2010), Subtropical cloud-regime transitions: Boundary layer depth and cloud-top height evolution in models and observations, *J. Appl. Meteorol. Climatol.*, *49*, 1845–1858, doi:10.1175/2010JAMC2338.1.

Liang, C. K., A. Eldering, F. W. Irion, W. G. Read, E. J. Fetzer, B. H. Kahn, and K.-N. Liou (2010), Characterization of merged AIRS and MLS water vapor sensitivity through integration of averaging kernels and retrievals, *Atmos. Meas. Tech. Discuss.*, *3*, 2833–2859, doi:10.5194/amtd-3-2833-2010.

Maddy, E. S., and C. D. Barnet (2008), Vertical resolution estimates in version 5 of AIRS operational retrievals, *IEEE Trans. Geosci. Remote Sens.*, *46*(8), 2375–2384, doi:10.1109/TGRS.2008.917498.

Nuijens, L., B. Stevens, and A. P. Siebesma (2009), The environment of precipitating shallow cumulus convection, *J. Atmos. Sci.*, *66*(7), 1962–1979, doi:10.1175/2008JAS2841.1.

Pougatchev, N. (2008), Validation of atmospheric sounders by correlative measurements, *Appl. Opt.*, *47*(26), 4739–4748.

Rauber, R. M., et al. (2007), Rain in shallow cumulus over the ocean: The RICO campaign, *Bull. Am. Meteorol. Soc.*, *88*(12), 1912–1928, doi:10.1175/BAMS-88-12-1912.

Riehl, H., T. C. Yeh, J. S. Malkus, and N. E. Laseur (1951), The north-east trade of the Pacific Ocean, *Q. J. R. Meteorol. Soc.*, *77*(334), 598–626, doi:10.1002/qj.49707733405.

Siebesma, A. P., et al. (2003), A large eddy simulation intercomparison study of shallow cumulus convection, *J. Atmos. Sci.*, *60*(10), 1201–1219, doi:10.1175/1520-0469(2003)60<1201:ALESIS>2.0.CO;2.

Snodgrass, E. R., L. Di Girolamo, and R. M. Rauber (2009), Precipitation characteristics of trade wind clouds during RICO derived from radar, satellite, and aircraft measurements, *J. Appl. Meteorol. Climatol.*, *48*, 464–483, doi:10.1175/2008JAMC1946.1.

Stevens, B. (2005), Atmospheric moist convection, *Annu. Rev. Earth Planet. Sci.*, *33*, 605–643, doi:10.1146/annurev.earth.33.092203.122658.

Susskind, J., C. Barnet, J. Blaisdell, L. Iredell, F. Keita, L. Kouvaris, G. Molnar, and M. Chahine (2006), Accuracy of geophysical parameters derived from Atmospheric Infrared Sounder/Advanced Microwave Sounding Unit as a function of fractional cloud cover, *J. Geophys. Res.*, *111*, D09S17, doi:10.1029/2005JD006272.

Susskind, J., J. M. Blaisdell, L. Iredell, and F. Keita (2010), Improved temperature sounding and quality control methodology using AIRS/AMSU data: The AIRS Science Team Version 5 retrieval algorithm, *IEEE Trans. Geosci. Remote Sens.*, *PP*(99), 1–25, doi:10.1109/TGRS.2010.2070508.

Teixeira, J., et al. (2008), Parameterization of the atmospheric boundary layer, *Bull. Am. Meteorol. Soc.*, *89*(4), 453–458, doi:10.1175/BAMS-89-4-453.

von Engeln, A., J. Teixeira, J. Wickert, and S. A. Buehler (2005), Using CHAMP radio occultation data to determine the top altitude of the Planetary Boundary Layer, *Geophys. Res. Lett.*, *32*, L06815, doi:10.1029/2004GL022168.

Wilks, D. S. (1995), *Statistical Methods in the Atmospheric Sciences: An Introduction*, 464 pp., Academic, San Diego, Calif.

Wood, R., and C. S. Bretherton (2004), Boundary layer depth, entrainment, and decoupling in the cloud-capped subtropical and tropical marine boundary layer, *J. Clim.*, *17*(18), 3576–3588, doi:10.1175/1520-0442(2004)017<3576:BLDEAD>2.0.CO;2.

Wu, L. (2009), Comparison of atmospheric infrared sounder temperature and relative humidity profiles with NASA African Monsoon Multidisciplinary

Analyses (NAMMA) dropsonde observations, *J. Geophys. Res.*, *114*, D19205, doi:10.1029/2009JD012083.
Wyant, M. C., C. S. Bretherton, J. T. Bacmeister, J. T. Kiehl, I. M. Held, M. Zhao, S. A. Klein, and B. J. Soden (2006), A comparison of low-latitude cloud properties and their response to climate change in three AGCMs sorted into regimes using mid-tropospheric vertical velocity, *Clim. Dyn.*, *27*(2–3), 261–279, doi:10.1007/s00382-006-0138-4.
Zuidema, P., D. Painemal, S. de Szoeke, and C. Fairall (2009), Stratocumulus cloud-top height estimates and their climatic implications, *J. Clim.*, *22*(17), 4652–4666, doi:10.1175/2009JCLI2708.1.

V. T. Dang, E. J. Fetzer, E. Fishbein, F. W. Irion, B. H. Kahn, and J. Teixeira, Jet Propulsion Laboratory, California Institute of Technology, 4800 Oak Grove Dr., Pasadena, CA 91109, USA.

J. P. A. Martins, P. M. A. Miranda, and P. M. M. Soares, CGUL, IDL, University of Lisbon, Edificio C8, Piso 3, Sala 8.8.32, Lisbon 1749-016, Portugal. (joaopam@gmail.com)